

Review

## Phase Competitions behind the Giant Magnetic Entropy Variation: $Gd_5Si_2Ge_2$ and $Tb_5Si_2Ge_2$ Case Studies

Ana Lúcia Pires<sup>1,2,†</sup>, João Horta Belo<sup>1,†</sup>, Armandina Maria Lima Lopes<sup>1,2</sup>, Isabel T. Gomes<sup>1</sup>, Luis Morellón<sup>3</sup>, Cesar Magen<sup>3,4</sup>, Pedro Antonio Algarabel<sup>5</sup>, Manuel Ricardo Ibarra<sup>3</sup>, André Miguel Pereira<sup>1,\*</sup> and João Pedro Araújo<sup>1,\*</sup>

<sup>1</sup> IFIMUP and IN—Institute of Nanoscience and Nanotechnology, Departamento de Física e Astronomia da Faculdade de Ciências da Universidade do Porto, Rua do Campo Alegre, 687, Porto 4769-007, Portugal; E-Mails: pires.analuci@gmail.com (A.L.P.); joao.horta.belo@gmail.com (J.H.B.); Armandina.Lima.Lopes@cern.ch (A.M.L.L.); itarroso@gmail.com (I.T.G.)

<sup>2</sup> CFNUL—Centro de Física Nuclear da Universidade de Lisboa, Av. Prof. Gama Pinto, 2, Lisboa 1649-003, Portugal

<sup>3</sup> Instituto de Nanociencia de Aragón, Universidad de Zaragoza, ES-50018 Zaragoza, Spain and Departamento de Física de la Materia Condensada, Universidad de Zaragoza, Zaragoza 50009, Spain; E-Mails: morellon@unizar.es (L.M.); cmagend@gmail.com (C.M.); ibarra@unizar.es (M.R.I.)

<sup>4</sup> Fundación ARAID, Zaragoza 50018, Spain

<sup>5</sup> Instituto de Ciencia de Materiales de Aragón, CSIC-Universidad de Zaragoza, and Departamento de Física de la Materia Condensada, Universidad de Zaragoza, Zaragoza 50009, Spain; E-Mail: algarabe@unizar.es

† These authors contributed equally to this work.

\* Authors to whom correspondence should be addressed; E-Mails: ampereira@fc.up.pt (A.M.P.); jearaujo@fc.up.pt (J.P.A.); Tel.: +351-22 04 02 362.

Received: 11 April 2014; in revised form: 27 June 2014 / Accepted: 1 July 2014 /

Published: 11 July 2014

---

**Abstract:** Magnetic materials with strong spin-lattice coupling are a powerful set of candidates for multifunctional applications because of their multiferroic, magnetocaloric (MCE), magnetostrictive and magnetoresistive effects. In these materials there is a strong competition between two states (where a state comprises an atomic and an associated magnetic structure) that leads to the occurrence of phase transitions under subtle variations of external parameters, such as temperature, magnetic field and hydrostatic pressure. In this review a general method combining detailed magnetic measurements/analysis and first

principles calculations with the purpose of estimating the phase transition temperature is presented with the help of two examples ( $\text{Gd}_5\text{Si}_2\text{Ge}_2$  and  $\text{Tb}_5\text{Si}_2\text{Ge}_2$ ). It is demonstrated that such method is an important tool for a deeper understanding of the (de)coupled nature of each phase transition in the materials belonging to the  $\text{R}_5(\text{Si,Ge})_4$  family and most possibly can be applied to other systems. The exotic Griffiths-like phase in the framework of the  $\text{R}_5(\text{Si}_x\text{Ge}_{1-x})_4$  compounds is reviewed and its generalization as a requisite for strong phase competitions systems that present large magneto-responsive properties is proposed.

**Keywords:** entropy; phase transitions; magnetocaloric effect

**PACS Codes:** 65.40.gd; 75.30.Kz; 75.30.Sg

## 1. Introduction

Back in the 1980s, the simultaneous discovery of the “ozone hole” in the stratosphere and of the influence of the emission of CFC gases, widely used in every refrigeration system at that time, in the thinning of the ozone layer triggered the search for alternative refrigeration technologies in order to replace the gas-compression technology [1]. The thermoelectric and thermomagnetic technologies are ahead in this race. Here only the latter one will be discussed and in particular the nature of the effect behind this technology—the magnetocaloric effect (MCE). The MCE was first observed in the 1840s, when Joule observed a temperature variation in a sample of pure iron as it was subjected to a magnetic field change [2]. It was understood on the basis of thermodynamics by Weiss and Piccard in 1917 [2]. At that time it became clear that the MCE is a phenomenon occurring in all magnetic materials when subjected to magnetic field variations, originating from the energy/entropy exchange between the magnetic and atomic lattice reservoirs. Through the fundamental Maxwell relations, the MCE can be expressed as the adiabatic temperature ( $\Delta T_{ad}$ ) and the isothermal magnetic entropy ( $\Delta S_{iso}^m$ ) variation that a magnetic material undergoes when varying an external magnetic field [3]:

$$\Delta T_{ad}(S, \Delta H)_{\Delta H} = -\mu_0 \int_{H_0}^{H_1} \left( \frac{T}{C(T, H)} \right)_H \left( \frac{\partial M(T, M)}{\partial T} \right)_H dH \quad (1)$$

$$\Delta S_{iso}^m(T, \Delta H)_{\Delta H} = \mu_0 \int_{H_0}^{H_1} \left( \frac{\partial M(T, M)}{\partial T} \right)_H dH \quad (2)$$

where  $T$  is the temperature of the material,  $\Delta H = H_1 - H_0$  is the magnetic field variation,  $C$  is the heat capacity and  $M$  the magnetization. Hence, in order to maximize  $\Delta T$  and  $\Delta S$ , one important parameter to consider is the magnetization variation as a function of temperature: this means that the MCE reaches its maximum at the magnetic transition temperatures (the Curie temperature  $T_C$ , or the Néel temperature  $T_N$ ) for all magnetic materials and consequently the operational temperature range of each material is delimited by a small interval close to its magnetic transition temperature. Furthermore, the MCE maximization depends strongly on the value of the magnetization derivative with respect to temperature  $\partial M/\partial T$ , which is specific for each material and depends on the order of the associated phase transition.

Still in the 1930s, Giauque understood that he could make use of the large magnetization change at low temperatures of a paramagnetic salt (particularly gadolinium sulphate) to reach sub-Kelvin temperatures for the first time [4] and for a long time magnetic refrigeration was only considered for low temperature applications. Forty years later, in 1973, Brown [5] used gadolinium (which has a  $T_C$  around 295 K) to design a magnetic refrigerator capable of operating at room temperature [6,7]. However, the real drive towards room temperature magnetic refrigeration occurred with the aforementioned events during the 1980s [1]. Finally, in 1997, Pecharsky and Gschneidner discovered the reversible giant magnetocaloric effect (GMCE) in the compound  $Gd_5Si_2Ge_2$  [8], renewing the optimism in this technology and attracting the attention of materials scientists from different areas to its study. They indirectly measured an entropy change of  $18 \text{ J Kg}^{-1} \text{ K}^{-1}$  at 278 K for a field change of 0–5 T [8]. Later, Morellon and co-workers [9] discovered that the origin of such a giant effect is the simultaneous magnetic and structural (magnetostructural) transition that  $Gd_5Si_2Ge_2$  undergoes at 278 K and that can also be triggered by the application of a magnetic field. The magnetostructural transition ensures a first-order nature of the magnetic transition and it is the reason for the giant  $\partial M/\partial T$  value and consequently for the maximization of  $\Delta S^m$ . Moreover, since a magnetostructural transition occurs, it is important to consider the additional entropy change contribution due to the structural transition,  $\Delta S^{str}$  [10]. Since  $\Delta S^m$  accounts for the purely magnetic driven processes, the total entropy variation is:  $\Delta S^t = \Delta S^m + \Delta S^{str}$ . Because of the reasons mentioned above it became clear that first-order magnetostructural transitions are a requirement for the GMCE, and very rapidly several materials were found that fulfill this requirement, such as NiMnGa [11]; NiMnInCo [12]; MnCoGeB [13], MnFePGe [14] and MnAs [15]. There are other materials presenting GMCE, that do not exhibit any structural transition (in the sense that their symmetry group does not change), yet still undergo large simultaneous changes in their unit cell volume and in their magnetization, as for instance  $La(FeSi)_{13}$  [16],  $La(FeSi)_{13}H$  [17] and  $LaCaMnO_3$  [18]. It was found that materials undergoing magnetostructural/magnetovolume transitions provide other giant magneto-responsive properties with technological interest besides the giant magnetocaloric effect, such as giant magnetostriction [19] and magnetoresistance [20]. It is important to remark that for these materials the magnetostriction is not a consequence of the reorientation of magnetic domains, as in the classical sense of magnetostriction, but instead it is a result of the structural transition induced by a magnetic field, which gives rise to sharp changes in the lattice parameters and consequently to macroscopic shape and/or volume changes of the material.

Thus, magnetostructural transitions have been attracting an increasing number of scientists, from both experimental and theoretical backgrounds, due to the multifunctionality arising from these effects. In systems exhibiting magnetostructural transitions there is a strong competition between the magnetic and crystallographic degrees of freedom involved in the transition, which is very sensitive to extrinsic parameters—such as temperature, magnetic field, pressure—and intrinsic properties—disorder (chemical and strain) and microstructure [1,21–24]. It is very difficult to theoretically predict the influence of intrinsic properties, but the effect of external parameters, such as magnetic field and temperature, can be predicted. In 2006, Paudyal and co-workers [25] developed a pioneering work based on the fundamental thermodynamic equations and on results from first principles calculations, which allowed the theoretical estimation of the temperature dependencies of several magnetic properties (including the MCE) of the  $Gd_5Si_2Ge_2$  compound. They were able to plot the free energies of both structures in competition as a function of temperature and from the behavior of these curves they were able to

estimate whether there is a magnetostructural transition, as well as the temperature at which it occurs. Recently, the same approach was extended to the  $\text{Tb}_5(\text{Si,Ge})_4$  system allowing a better understanding on the (de)coupled nature of the magnetic and structural transitions [26,27]. Moreover, first principles calculations have also shown to be a fundamental tool to understand the correlation between electronic and magnetic interactions within the unit cell of the  $\text{R}_5(\text{Si,Ge})_4$  compounds [26,28].

It is noteworthy that whether there is a magnetostructural transition or not is a critical feature both from the scientific point of view, in order to understand the origins of such large magnetic responses such as the magnetocaloric, magnetoresistive and magnetostrictive effects, but also technologically, since the occurrence of a magnetostructural transition promotes a giant enhancement on the magnitude of all these effects and specially the MCE. This statement is very patent in the Gschneidner and co-workers report where they show that  $\Delta S^{\text{str}}$  can account for more than half of the total entropy variation for applied magnetic fields below 2 T in  $\text{Gd}_5(\text{Si,Ge})_4$  compounds and its contribution can be even higher for other compounds. This means that for materials where no magnetostructural transition is observed, in principle it should be possible to greatly optimize their MCE through the strengthening of their magnetic and structural coupling. Simultaneously, it also means that for materials where a magnetostructural transition is observed, the path to optimize their MCE should not be focused in increasing their magnetic and structural coupling.

In this review we will focus on the nature of a first order magnetic transition from the point of view of a competition between two crystallographic phases. The thermodynamic framework will be introduced in combination with first principles calculations. Afterwards we will discuss the importance of knowing the magnetic transition temperatures of both phases involved and a general method to estimate their values through simple experimental measurements. The practical cases of  $\text{Gd}_5\text{Si}_2\text{Ge}_2$  and  $\text{Tb}_5\text{Si}_2\text{Ge}_2$  will be presented to explain the (de)coupling of the magnetic and structural phase transitions in both compounds. By incorporating the aforementioned external parameters, the plots of the free energy as a function of temperature will be presented and the effect of an applied magnetic field will be discussed. Finally, the correlation between this phase competition and one exotic phenomenon—the Griffiths-like phase—will also be discussed and presented as a fingerprint of systems with strong competition between phases.

## 2. Thermodynamics of First Order Phase Transitions

### 2.1. General Approach

According to the Ehrenfest classification, a first order phase transition must exhibit a discontinuity in the entropy variation and in the order parameter which arises from a crossover between two free energies, resulting in two distinct states: a low temperature (LT) and a high temperature (HT) state. It is the change between these two states that leads to the discontinuity of the entropy and the maximization of the entropy variation, leading to a giant magnetocaloric effect in the case of magnetic materials. Besides temperature, it is crucial that the application/removal of the external parameters (pressure, magnetic field, *etc.*) can be made near the phase transition region to be able to modify the system. To understand this process thermodynamically, let us consider the free energy for a simple magnetic material [25]:

$$F(T, \sigma) = U - TS = U^{\text{lattice}} - HgJ\sigma - \frac{3}{2} \frac{J}{J+1} k_B T_C \sigma^2 - TS^m - TS^{\text{lattice}} \quad (3)$$

where  $\sigma$  is the reduced magnetization, the first term ( $U^{\text{lattice}}$ ) is the non-magnetic internal energy at  $T = 0$  K, the second term is the interaction energy between a localized magnetic moment  $J$  and the applied magnetic field  $H$  (Zeeman term), the third one is the magnetic ion-ion exchange interaction energy and the last two terms are the entropic contributions (magnetic and lattice, respectively) to the system's free energy.

With the help of first principles calculations, one can estimate the free energy of any structure and, in particular, of any two structures (say 1 and 2) involved in a structural transition  $1 \rightarrow 2$  (where 1 and 2 correspond to the HT and LT magnetization states, respectively):  $\Delta F = F[1] - F[2]$ . This will be equal to the difference between the  $U^{\text{lattice}}$  of both structures at  $T = 0$  K and  $H = 0$  T, which are estimated from first principles calculations. Considering the mean field theory, the magnetic entropy per magnetic ion ( $S_M$ ) for a general  $J$  can be estimated from:

$$S_M(\sigma) = k_B \ln \left( \frac{\sinh\left(\frac{2J+1}{2J} B_J^{-1}(\sigma)\right)}{\sinh\left(\frac{1}{2J} B_J^{-1}(\sigma)\right)} \right) - \sigma B_J^{-1}(\sigma) \sim k_B \left[ \ln(2J+1) - \frac{3}{2} \frac{J}{J+1} \sigma^2 + O(\sigma^4) \right] \quad (4)$$

where  $B_J^{-1}$  is the inverse Brillouin function. The magnetic equation of state ( $\sigma(T, H)$ ) can be obtained by finding the zero of the derivative of Equation (3) with respect to  $\sigma$  [leading to  $\sigma = \sigma(T, H)$ ], which corresponds to the condition of minimum free energy. This minimum free energy is then given by  $F^{\text{min}}(T, H) = F(T, \sigma(T, H))$ . From Equation (3) one can see that the free energy difference between structures 1 and 2 arises from a) the non-magnetic contribution ( $F_{\text{lattice}} = U^{\text{lattice}} - TS^{\text{lattice}}$ ) and b) from the exchange and magnetic entropy terms (2nd, 3rd and 4th terms in Equation (3)), given the hypothetically different  $T_C$  of the two structures. Therefore it becomes critically important to know the  $T_C$  of each structure involved in order to be able to plot the free energies of both structures as a function of temperature. Such a plot will allow one to understand whether or not there is a structural transition occurring and, if so, at what temperature it should occur. The first obstacle in this approximation is the determination of the magnetic ordering temperatures ( $T_C^1$  and  $T_C^2$ ) of both structures involved in a phase transition.

## 2.2. How to Inspect the "Hidden" Magnetic Ordering Temperatures

In standard materials exhibiting second-order magnetic transitions, their magnetic long range ordering sets in at a temperature that can be easily assessed by measuring their magnetization as a function of temperature at constant magnetic field, analysing its derivative and signalling the temperature at which a maximum/minimum occurs. Unfortunately, such a simple approach is not appropriate in systems presenting magnetostructural transitions, since in these systems the structural transition occurs somewhere in between  $T_C^1$  and  $T_C^2$ , *i.e.*,  $T_C^1 < T_S < T_C^2$ . Let us consider the  $M(T)$  measurement on cooling of such an ideal system. Starting with a low magnetization value associated with the paramagnetic state of structure 1, there will be no significant changes on  $M(T)$  when cooling through  $T_C^2$ . Then, when  $T = T_S$ , a sharp increase towards a much higher magnetization value will be

observed, which is already associated with the ferromagnetic behavior of structure 2. While continuing on cooling down the system, no major change will be observed in the  $M(T)$  curve, not even when crossing the lower Curie temperature of structure 1,  $T_C^1$ , because the system is already transformed into the structure 2. In conclusion, the  $T_C^1$  and  $T_C^2$  will be invisible to the  $M(T)$  measurement and that is why we have to figure out an alternative method to estimate  $T_C^1$  and  $T_C^2$ .

In order to be direct and clear, two practical examples will be considered. Both are materials presenting giant magnetocaloric effect:  $Gd_5Si_2Ge_2$ —with a simultaneous magnetic and structural transition—and  $Tb_5Si_2Ge_2$ —presenting non-simultaneous magnetic and structural transitions. Particularly for these two materials, the structures 1 and 2 mentioned above correspond to the monoclinic (M) and orthorhombic [O(I)] structures, whereas the two magnetic states considered are paramagnetic (PM) and ferromagnetic (FM). The remaining relevant information is summarized in Table 1.

**Table 1.** Relevant information about  $Tb_5Si_2Ge_2$  and  $Gd_5Si_2Ge_2$  compounds.

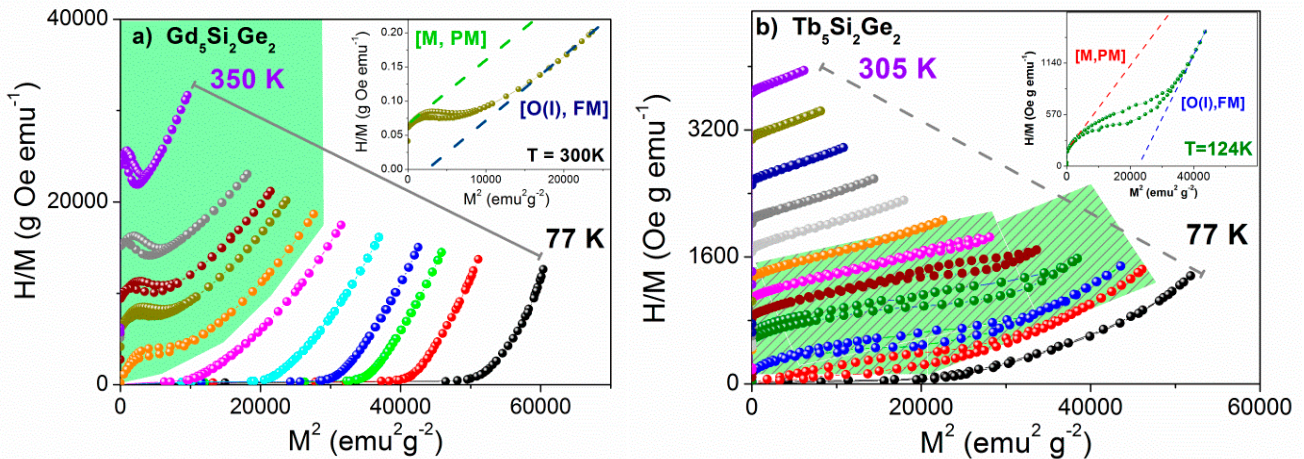
	$Tb_5Si_2Ge_2$	$Gd_5Si_2Ge_2$
Simultaneous transition	×	√
Structure 1/2	M/O(I)	M/O(I)
Curie temperatures, $T_C$ (K)	112/200 [27,29]	208/305 [25,27]
Structural transition temperature, $T_S$ (K)	95 [29]	270 [30,31]

Although these compounds were already thoroughly studied [8,23,32,33], in order to exemplify the broad range of application of this procedure, we will only take into account the fact that both materials undergo structural transitions under temperature and/or magnetic field changes. We will also assume that for both structures involved, the FM state is the most stable at low temperatures. Hence, with these assumptions, there are four different possible states:  $[M;PM^M]$ ,  $[M;FM^M]$ ,  $[O(I);PM^{O(I)}]$  and  $[O(I);FM^{O(I)}]$  at any temperature and field value. Now, let us consider that the temperature of the material ( $Tb_5Si_2Ge_2$  or  $Gd_5Si_2Ge_2$ ) is slightly above its structural transition temperature  $T_S$ , where the material stabilizes at its  $[M;PM^M]$  state. At this temperature it is possible to induce the magnetostructural transition, *i.e.*, the transition from the  $[M;PM^M]$  state to the  $[O(I);FM^{O(I)}]$  state through the application of a strong enough magnetic field (critical field,  $H_C$ ). Hence, for high magnetic fields ( $H > H_C$ ) it is possible to inspect the magnetic behavior of the O(I) structure, even at  $T > T_S$ . In fact, as expected, the critical field  $H_C$  depends on the temperature of the material and conversely the structural transition temperature  $T_S$  depends on the applied magnetic field intensity:  $T_S(H) \neq T_S \equiv T_S(H = 0)$ . Experimentally, such behavior can be more clearly understood in the isothermal magnetization curves as a function of applied field for several different temperatures (below and above  $T_S$ ). Two clearly distinct types of curves will be obtained: for  $T < T_S$  isotherms, a typical FM steep increase in the magnetization up to the saturation field is observed, whereas for  $T > T_S$  the magnetization exhibits two regimes: a low magnetization (LM) state at low fields undergoes a sharp metamagnetic transition into a high magnetization (HM) state at  $H > H_C$  as a consequence of the very different magnetic susceptibilities of structures M and O(I). The data are then represented in the form of Arrott plots [34]— $H/M$  as a function of  $M^2$ —, as can be seen in Figures 1a,b for  $Gd_5Si_2Ge_2$  and

Tb<sub>5</sub>Si<sub>2</sub>Ge<sub>2</sub>, respectively. This representation is based on the Landau theory of phase transitions and follows from the magnetic state equation [34]:

$$\frac{H}{M} = \alpha(T - T_C) + BM^2 \tag{5}$$

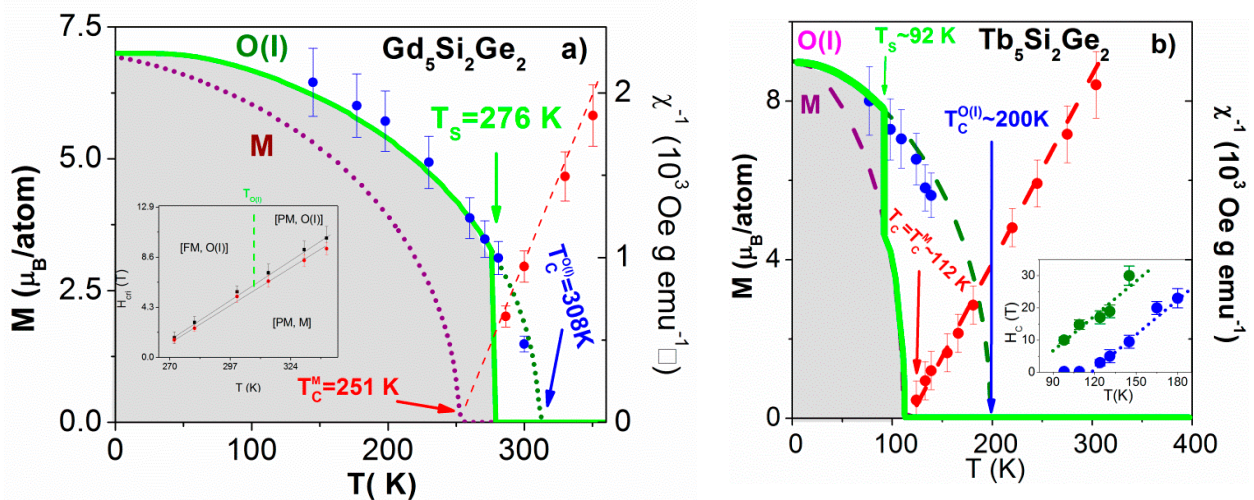
**Figure 1.** Arrott plots for Gd<sub>5</sub>Si<sub>2</sub>Ge<sub>2</sub> (a) in the temperature range 77–350 K; Inset: T = 300 K, and for Tb<sub>5</sub>Si<sub>2</sub>Ge<sub>2</sub> (b) in the temperature range of 77–305 K; Inset: T = 124 K.



From this expression one recognizes that when plotting the data in the  $H/M$  vs.  $M^2$  representation, linear curves are expected, intercepting the positive y-axis when  $T > T_C$  (in the PM state) and the positive x-axis when  $T < T_C$  (in the FM state). In this representation, the critical isotherm ( $T = T_C$ ) is a straight line that goes through the origin. The intercept with the positive y-axis,  $\alpha(T - T_C)$ , is the inverse susceptibility  $\chi^{-1}(T)$ . Let us consider the Gd<sub>5</sub>Si<sub>2</sub>Ge<sub>2</sub> case. As can be seen in Figure 1a, the curves in the green region exhibit two different linear regimes. This is a signature that they belong to the  $T_S(H) > T > T_S(H = 0)$  temperature range, where the magnetic field applied is able to induce the structural transition  $[M, PM^M] \rightarrow [O(I), FM^{O(I)}]$ .  $M$  has lower magnetic susceptibility (smoother slope) than the  $O(I)$  structure (steeper slope) (inset of Figure 1a). Now, the squared spontaneous magnetization  $M_s^2 [O(I)]$  of the  $O(I)$  structure (or HM state) can be estimated as the interception of the linear extrapolation of the high field magnetization data with the abscissa axis at a fixed temperature. In the white region— $T < T_S$  temperature range—only one linear regime is observed because the system is already in the  $[O(I), FM^{O(I)}]$  state. By following the same procedure, the  $M_s^2 [O(I)]$  values at lower temperatures are estimated. By combining the  $M_s^2 [O(I)]$  values obtained for  $T < T_S$  and for  $T > T_S$ , it is possible to plot  $M_s^2 [O(I)]$  as a function of temperature as depicted in Figure 2a (blue dots). Simultaneously, the inverse paramagnetic susceptibility of the  $M$  structure (LM state) can also be determined from the low field isothermal curves ( $T > T_S$ ) and their intercept with the positive y-axis, yielding  $\chi^{-1}[M](T)$ , which is also displayed in Figure 2a (red dots). Finally, by fitting the  $M_s^2 [O(I)](T)$  and the  $\chi^{-1}[M](T)$  curves with Brillouin and linear functions, respectively, it is possible to estimate the Curie temperatures of both  $M$  and  $O(I)$  phases. In this example the fits result in the following critical temperatures for  $O(I)$  and  $M$  structures:  $T_C^{O(I)} \sim 308$  K and  $T_C^M \sim 251$  K, in accordance with previous results [25,27,35,36]

The Arrott plots for  $\text{Tb}_5\text{Si}_2\text{Ge}_2$  are shown in Figure 1b. As in the  $\text{Gd}_5\text{Si}_2\text{Ge}_2$  plots, the green area highlights the temperature range where the magnetic field is able to induce the M to O(I) phase transition. At  $T = 124$  K (inset of Figure 1b), the behavior of the curves signals the magnetostructural transition from the LM [M,  $\text{PM}^M$ ] to the HM [O(I),  $\text{FM}^{\text{O(I)}}$ ] state. Following the same procedure as in the  $\text{Gd}_5\text{Si}_2\text{Ge}_2$  case, the data analysis allows extracting the temperature dependence of both the inverse paramagnetic susceptibility of the M structure (red dots in Figure 2b) and the spontaneous magnetization of the O(I) structure (blue dots in Figure 2b). Again, by fitting these data, the extracted values are:  $T_C^{\text{O(I)}} \sim 200$  K and  $T_C^M \sim 112$  K, where the latter one is coincident with the  $T_C \sim 112$  K obtained from the maximum derivative of the experimentally measured  $M(T)$  curves [29].

**Figure 2.** Spontaneous magnetization (blue dots) and reciprocal susceptibility (red dots) curves of: (a)  $\text{Gd}_5\text{Si}_2\text{Ge}_2$  and (b)  $\text{Tb}_5\text{Si}_2\text{Ge}_2$ , obtained from the Arrott plots. The dark green dotted lines are the Brillouin fits to the spontaneous magnetization of the O(I) structure for each compound which enable the estimation of their  $T_C$ :  $T_C^{\text{O(I)}} = 308$  K for  $\text{Gd}_5\text{Si}_2\text{Ge}_2$  and  $T_C^{\text{O(I)}} = 200$  K for  $\text{Tb}_5\text{Si}_2\text{Ge}_2$ . The red dashed lines are the linear fits to the reciprocal susceptibility data, which allowed estimating the  $T_C^M$  for each compound:  $T_C^M = 251$  K for  $\text{Gd}_5\text{Si}_2\text{Ge}_2$  and  $T_C^M = 112$  K for  $\text{Tb}_5\text{Si}_2\text{Ge}_2$ , whereas the purple dotted lines represent the Brillouin curves assuming the obtained  $T_C^M$ . The gray zones represent the FM regions and their boundaries (represented by the light-green curves) schematically represent the experimentally measured  $M(T)$  curves. Insets: temperature dependence of the critical magnetic fields ( $H_C(T)$ ) obtained from the maximum of  $dM/dH$ .



In summary, the general procedure to extract the “hidden” magnetic ordering temperatures of structures 1 and 2 is as follows:

- (1) Measure the magnetization as a function of magnetic field for several temperatures in the range where  $T_S$  is expected (a broader interval will provide more points and hence more accurate fits), ensuring that for some isotherms the field is strong enough to induce the metamagnetic transition;
- (2) Replot the data in the Arrott form ( $H/M$  as a function of  $M^2$ ) and identify the two different linear regimes associated with LM (1) and HM (2) states for  $T > T_S$ ;

- (3) Perform linear fits to these two different regimes and estimate their interceptions with the positive y-axis (for the LM state) and with the positive x-axis (for the HM state) in order to extract, respectively, the inverse susceptibility of the LM (1) state— $\chi^{-1}(\text{LM})$ —and the squared spontaneous magnetization of the HM (2) phase— $M_s^2(\text{HM})$ ;
- (4) Plot  $\chi^{-1}(1)$  and  $M_s^2(2)$  as a function of temperature;
- (5) Through linear and Brillouin fits to these curves, the magnetic ordering temperatures of both 1 and 2 structures are extracted.

To the best of our knowledge, this procedure has only been applied to the  $R_5(\text{Si,Ge})_4$  family of compounds. However, it could be useful for studying several other materials displaying magnetic field-induced structural transitions, hence with extremely sensitive magneto-responsive properties that are attractive for technological applications. Examples of such materials are the multifunctional magnetic shape memory alloy  $\text{Ni}_{55}\text{Mn}_{20}\text{Ga}_{25}$  [11], the  $\text{MnNiFeGe}$  family [12],  $\text{MnCoGeB}$  [13],  $\text{MnFePGe}$  [14], and the materials undergoing giant volume changes within the same crystallographic structure:  $\text{La-Fe-Si}$  [16] and  $\text{LaCaMnO}_3$  [18].

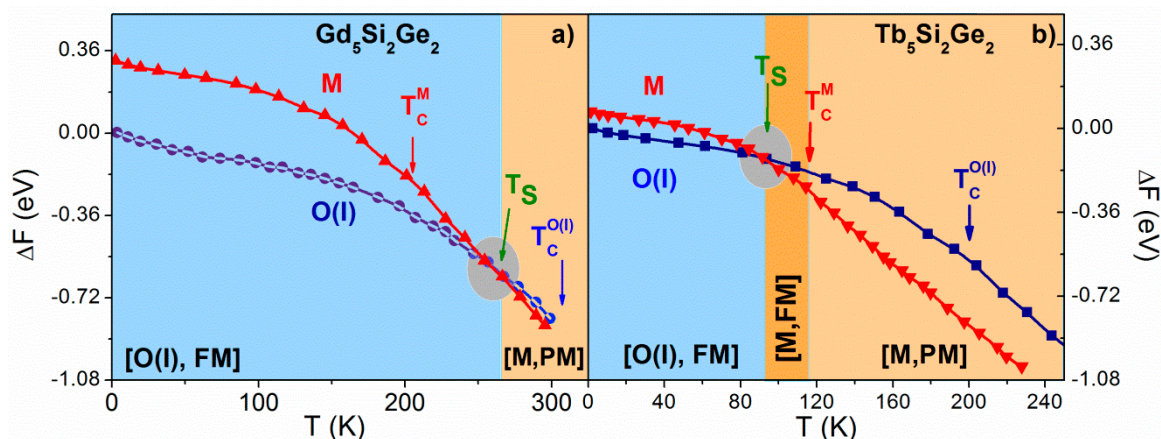
### 2.3. Free Energy Crossings of Real Systems

Once the  $T_C$  of both structures is estimated from the Arrott plots using the method described above, their free energies can be calculated as a function of temperature. Then, the temperature at which the free energy curves of both structures intersect will define the structural transition temperature  $T_S$ . As a first approximation, we neglect the lattice entropy term and consider the magnetic contribution to the free energy in Equation (3), as well as the result of first principles calculations that yields  $F_{\min}^{\text{lattice}}(T = 0\text{K}) = U^{\text{lattice}}$  (the first term in Equation (3)). In order to normalize the energy range to zero, the value of the free energy at 0 K of structure 2 is subtracted from the free energy  $F_{\min}^{\text{lattice}}$  of both structures, resulting in:  $\Delta F_{\min}(T)[1,2] = F_{\min}(T)[1,2] - F_{\min}^{\text{lattice}}(T = 0\text{K})[2]$ . Let us start with a zero magnetic field, meaning that the second term in Equation 3 is also zero. The temperature dependence of the magnetic free energies  $\Delta F_{\min}[1]$  and  $\Delta F_{\min}[2]$  (that start at zero because of the subtraction mentioned above) are represented for the two examples  $\text{Gd}_5\text{Si}_2\text{Ge}_2$  and  $\text{Tb}_5\text{Si}_2\text{Ge}_2$  in Figures 3a,b, respectively. We recall that structure 1 corresponds to the monoclinic (M) crystallographic phase and structure 2 corresponds to orthorhombic O(I) phase. The first principles calculations were performed using Wien2K code, via the augmented plane wave method with local orbitals (APW + lo) and using the local spin-density approximation method allowing a correct estimation of the free energies of the M and O(I) phase at  $T = 0$  K.

It can be clearly seen that in both cases there is an intersection of the  $\Delta F_{\min}[\text{O(I)}]$  and  $\Delta F_{\min}[\text{M}]$  curves at a temperature  $T = T_S$ , *i.e.*, the structural transition temperature for each system. In the  $\text{Gd}_5\text{Si}_2\text{Ge}_2$  case (Figure 3a),  $T_S \sim 265$  K lies right between the two magnetic transition temperatures,  $T_C^{\text{M}} < T_S < T_C^{\text{O(I)}}$ , which means that upon cooling the system undergoes simultaneously a magnetic—paramagnetic to ferromagnetic  $[\text{PM}^{\text{M}}] \rightarrow [\text{FM}^{\text{O(I)}}]$ —and a structural transition from a monoclinic to an orthorhombic O(I) structure  $[\text{M}] \rightarrow [\text{O(I)}]$ . It is worth noting that, magnetically, the system goes from the monoclinic paramagnetic state to the orthorhombic ferromagnetic state, *i.e.*, there is a large discontinuity on both the atomic and lattice parameters and the magnetization values and these two transitions are coupled, meaning that a magnetostructural transition  $[\text{M}, \text{PM}^{\text{M}}] \rightarrow [\text{O(I)}, \text{FM}^{\text{O(I)}}]$ ,

$\text{FM}^{\text{O(I)}}$ ] takes place. In the case of  $\text{Tb}_5\text{Si}_2\text{Ge}_2$ ,  $T_S < T_C^M < T_C^{\text{O(I)}}$ , meaning that on cooling the system first undergoes the  $[\text{PM}^M] \rightarrow [\text{FM}^M]$  magnetic transition at  $T_C^M \sim 112$  K, closely followed by the  $M \rightarrow \text{O(I)}$  structural transition a few kelvins below, at  $T_S \sim 95$  K, *i.e.*, the two transitions are decoupled. In contrast with  $\text{Gd}_5\text{Si}_2\text{Ge}_2$ , here the magnetic transition is from the PM to the FM state of the monoclinic structure. The  $T_S$  values estimated with this theoretical model corroborate the values obtained from experimental measurements (particularly X-ray diffraction as a function of temperature) for these two compounds [29,30]. This demonstrates that such theoretical procedure can predict structural transition temperatures and their coupled/decoupled nature. As mentioned in the introduction section, this information is of key importance, since it allows evaluating the potential of the material regarding the optimization of its MCE. In particular, from the results of the two cases presented here it becomes clear that: (1) the MCE in  $\text{Tb}_5\text{Si}_2\text{Ge}_2$  can still be greatly increased, whereas (2)  $\text{Gd}_5\text{Si}_2\text{Ge}_2$  MCE cannot be improved much further by the further enhancement of its magnetic and structural coupling. Two of the most common ways to enhance this coupling is by applying pressure and by alloying. So far, our predictions have been confirmed by several works: concerning: (1), an MCE enhancement of more than 40% was reported by promoting the fully coupled magnetic and structural transitions, both by alloying with Fe [37] and by applying pressure [24], whereas regarding (2), the MCE was not improved (in fact it was smaller) when the same alloying and pressure were applied [38,39].

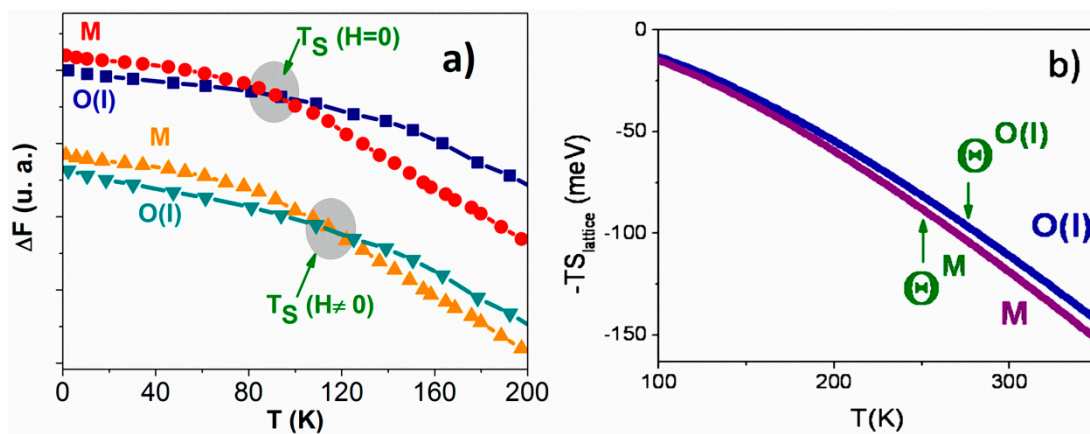
**Figure 3.** Free energy as a function of temperature considering the magnetic entropy and the first principles calculations ( $U^{\text{lattice}}$ ) for both M and O(I) structures in the (a)  $\text{Gd}_5\text{Si}_2\text{Ge}_2$  and (b)  $\text{Tb}_5\text{Si}_2\text{Ge}_2$  materials.  $T_S$  is defined as the temperature at which the crossing  $\Delta F_{\text{min}}[\text{M}] = \Delta F_{\text{min}}[\text{O(I)}]$  occurs.



The  $T_C^M < T_S < T_C^{\text{O(I)}}$  scenario, or more generally  $T_C^1 < T_S < T_C^2$ , is more attractive from the magnetic entropy change maximization point of view. As previously discussed by Liu [40], Pecharsky, Gschneidner and co-workers [21,41], the magnetic entropy change peak ( $\Delta S_{\text{max}}^m$ ) will be higher for systems where simultaneously  $\Delta T_C = T_C^2 - T_C^1$  is maximized and  $T_S$  is just slightly above  $T_C^1$ . In this scenario, the magnetization will jump ( $\Delta M$ ) from a nearly zero value to almost the maximum value of the magnetization of structure 2 ( $\Delta M$  will be proportional to the difference  $\Delta T_{CS} = T_C^2 - T_S$ ), hence maximizing the  $\partial M / \partial T$  at  $T_S$  and consequently the  $\Delta S_{\text{max}}^m$ .

Now, let us turn on the magnetic field. As can be seen in Equation (3), the second term ( $HgJ\sigma$ ) is always positive, but it is preceded by a minus sign. Therefore, the effect of a non-zero magnetic field is to lower the free energy. However, due to the different  $T_C$  on each crystal structure (that critically influence the magnetization  $\sigma(T_C)$ ), the free energy of the structure with higher  $T_C$  (O(I), in both materials) decreases more rapidly than the one with lower  $T_C$  (M). In this way the application of a magnetic field tends to increase the temperature at which the free energy crossover occurs—*i.e.*, where  $\Delta F_{\min}[O(I)] = \Delta F_{\min}[M]$ —as can be confirmed in Figure 4. Therefore, the structural transition temperature  $T_S(H)$  is increased. This was confirmed experimentally and a linear dependence of the critical magnetic field as a function of temperature  $H_C(T)$  was observed, as shown in the insets of Figure 2a,b.

**Figure 4.** (a) Schematic free energy of M and O(I) structures as a function of temperature for the zero (upper pair of curves) and non-zero (lower pair of curves) magnetic field; (b) Lattice contribution to the free energy of M and O(I) structures of  $Gd_5Si_2Ge_2$  compound as a function of temperature.



So far, the effect of  $F^{\text{lattice}} = TS^{\text{lattice}}$  was still not considered in this analysis. To analyze the contribution of the entropic lattice term, the Debye approximation is used. The entropy per ion is given by the following expression [40]:

$$\begin{aligned}
 S^{\text{lattice}}(\Theta) &= 3k_B \ln\left(1 - e^{-\frac{\Theta}{T}}\right) + 12k_B \left(\frac{T}{\Theta}\right)^3 \int_0^{\frac{\Theta}{T}} \frac{x^3}{e^x - 1} dx \\
 &\sim 3k_B \ln\left(\frac{\Theta}{T}\right) + \frac{3}{40}k_B \left(\frac{\Theta}{T}\right)^2 + O\left[\left(\frac{\Theta}{T}\right)^3\right]
 \end{aligned}
 \tag{6}$$

where  $\Theta$  is the (cut-off) Debye temperature. From this expression one can infer that the high temperature phase entropic contribution to the lattice free energy ( $-TS^{\text{lattice}}$ ) is lower for the structure with the lower  $\Theta$ . In fact, the Debye temperature for the M phase is lower than of the O(I) phase. This can be confirmed from the relation  $\frac{\Theta^M}{\Theta^{O(I)}} = \left(1 - \eta \frac{\Delta V}{V}\right)$ , where  $\eta$  is the Grüneisen parameter (typically around 10 for  $Gd_5Si_2Ge_2$ ) and  $\frac{\Delta V}{V}$  is the relative volume increase when the system goes through a O(I) to M structural change (typically  $\sim 1\%$ ). An estimation of  $\Theta^M$  considering the experimentally detected velocity of

sound in  $\text{Gd}_5\text{Si}_2\text{Ge}_2$  resulted in  $\Theta^{\text{M}} \sim 250$  K [42] and consequently  $\Theta^{O(I)} = \frac{\Theta^{\text{M}}}{\left(1 - \eta \frac{\Delta V}{V}\right)} \sim 278$  K. The

lower  $\Theta$  for the M phase was also experimentally confirmed in the case of  $\text{Y}_5(\text{Si}_x\text{Ge}_{1-x})_4$  system [43]. Furthermore, with the estimated  $\Theta$  for each structure of  $\text{Gd}_5\text{Si}_2\text{Ge}_2$  ( $\Theta^{\text{M}}$  and  $\Theta^{O(I)}$ ) it is possible to plot the lattice contribution from each structure to the free energy. This is displayed in Figure 4b. It can be seen in this figure that at high temperature the entropic lattice contribution also tends to stabilize the M phase, as shown for the  $\text{Y}_5(\text{Si}_x\text{Ge}_{1-x})_4$  system in [44]. Therefore it is clear, at least for these two examples, that including the lattice contribution ( $F^{\text{lattice}} = TS^{\text{lattice}}$ ) will not drastically affect the temperature dependence of the total free energy of each structure and, consequently, the main findings about the (de)coupled transition temperature discussed above.

However, the entropy change associated with the structural transition ( $\Delta S^{\text{str}}$ ) cannot be ignored, as it plays a major role on the total entropy variation ( $\Delta S^{\text{T}}$ ) of the majority of the systems undergoing magnetic field-induced structural transitions. As Pecharsky and Gschneidner [41] noticed, the lattice contribution to the total entropy change,  $\Delta S^{\text{str}}$ , varies from system to system because it depends on the entropy differences between both the initial and final structures. They also show that  $\Delta S^{\text{str}}$  is proportional to the volume difference between the two structures. Two examples are given:  $\Delta S^{\text{str}}$  is around 50% of  $\Delta S^{\text{T}}$  for the  $\text{Gd}_5\text{Si}_{2.09}\text{Ge}_{1.91}$  compound and about 93% of  $\Delta S^{\text{T}}$  for  $\text{MnCoGeB}_{0.2}$  under a magnetic field change of 5 T [41]. Furthermore, whereas the magnetic entropy change ( $\Delta S_{\text{max}}^{\text{m}}$ ) increases with  $H^{2/3}$  [45], the relation between  $\Delta S^{\text{str}}$  and  $H$  is harder to unveil. However, for these two systems a magnetic field change of 5 T is enough to complete the structural transition and hence  $\Delta S^{\text{str}}$  reaches its saturation value.

### 3. Is the Griffiths-like Phase a Requisite for a Giant Magnetocaloric Effect?

Together with the strong magneto-responsive properties, magnetic materials presenting strong coupling between structural and magnetic properties exhibit other exotic effects, such as the appearance of Griffiths-like phases. After the model proposed by Griffiths in the 1960s, the presence of Griffiths-like phases in several real materials has been recently reported [46]. In his model, Griffiths came upon with a diluted Ising ferromagnetic system with a well-defined magnetic ordering temperature  $T_{\text{C}}$  which was obviously lower than the magnetic ordering temperature of the undiluted (or pure) ferromagnetic system ( $T_{\text{G}}$ ), *i.e.*,  $T_{\text{C}} < T_{\text{G}}$ . He was able to show that for  $T_{\text{C}} < T < T_{\text{G}}$  it was possible that the reciprocal magnetic susceptibility of the system could deviate from its expected Curie-Weiss linear behavior. In fact, this deviation would start, on cooling, exactly at  $T_{\text{G}}$ , as if the diluted system somehow “remembered” that its magnetic ordering temperature was  $T_{\text{G}}$  “before” it became diluted [33]. Therefore, the concept of a Griffiths phase, also named Griffiths singularity, is based on the emergence of a new magnetic system within the paramagnetic matrix state, which evidences ferromagnetic short-range ordering [46–48]. Although these short-range clusters would not reveal themselves in the typical  $M(T)$  curves, they would be responsible for slight deviations from the linear behavior of the reciprocal magnetic susceptibility as a function of temperature.

In the past few years several  $\text{R}_5\text{T}_4$  compounds (R = rare earth: Gd, Tb, Dy, and Ho; T = group 14 elements) have shown a Griffiths-like behavior [33,48–50]. Such phenomenon was firstly reported in

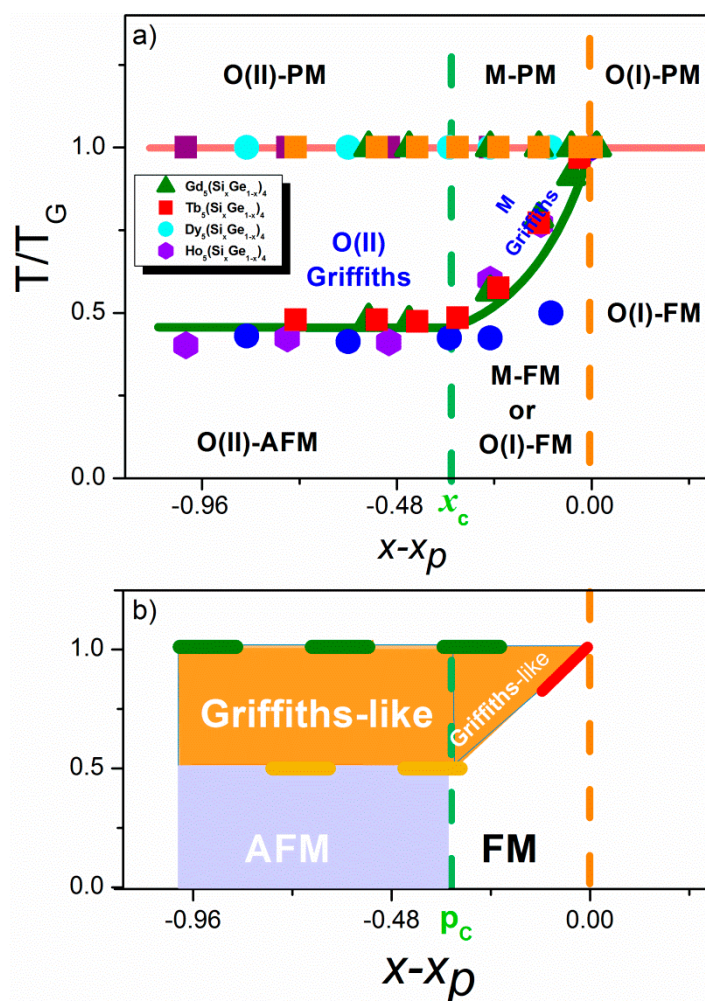
the  $\text{Tb}_5\text{Si}_2\text{Ge}_2$  compound, when it was associated with the experimentally observed deviation from the expected linearity (from Curie-Weiss law) of the  $\chi^{-1}(T)$  curve in the paramagnetic region,  $T > T_C$  [33].

Later, different works, reported by Ouyang, Tian, Pereira and co-workers identified the Griffiths-like phase in other compounds of the  $\text{R}_5\text{T}_4$  family [23,48–50]. All these compounds presented anomalies featuring their reciprocal susceptibility curve: a “stair-like” behavior occurring in an intermediate temperature region,  $T_C < T < T_G$ . Later on, our group has completed the phase diagrams of the  $\text{R}_5(\text{Si}_x\text{Ge}_{1-x})$  ( $\text{R} = \text{Gd}, \text{Tb}, \text{Dy}$  and  $\text{Ho}$ ) compounds with their corresponding Griffiths-like phase [50]. It was observed that despite the different main temperatures along their composition for each R compound ( $T_G$ ,  $T_C$  and  $T_N$ ), the phase diagrams were very similar in shape and two main conclusions could immediately be drawn: (1) the Griffiths singularity behavior appears only in the M and O(II) phases for compositions below a characteristic Si concentration that was defined as  $x_p$  and (2) the O(II) structure is stabilized when the ratio  $\tau \equiv T_{C,N} / T_G$  is  $\sim 0.5$ , regardless of the rare-earth element. The third and more general conclusion was reached when these diagrams were replotted as  $\tau$  as a function of  $(x-x_p)$  and the collapse of all four phase diagrams into a single curve was observed, as represented in Figure 5. The physical mechanism behind the appearance of the Griffiths-like phase is the same, regardless of the rare-earth element, and it is deeply associated with the Si/Ge ratio. In fact, the Ge substitution of Si makes a perfect analogy for the original undiluted/diluted system Griffiths idealized, *i.e.*, when no Ge is present or its concentration is such that  $x > x_p$  ( $x_p$  will be defined below), the system stabilizes in the O(I) structure where all interslab bonds are formed. A good review on the particular structural features of this system is given by Miller [1]. In the O(I) structure there is a strong and collinear ferromagnetic state with the highest  $T_C$  for each phase diagram—the system can be thought of as undiluted/pure. When the Ge substitution leads to a Si critical concentration ( $x_p$  is defined as this Si concentration value) the interslab bonds start to break (it is hypothesized that it is when  $x = x_p$  that the Ge atoms start substituting Si atoms at the interslab sites) and the O(II) or M structures become the most stable structures, with a simultaneous decrease in  $T_C$ . In these conditions the system can be thought of as diluted. It is well-known from previous studies that the magnetism in these compounds exists from the competition of ferromagnetic (within each slab) and antiferromagnetic interactions (mostly between slabs). More accurately, at the interslab region, the main magnetic exchange mechanism is the Ruderman-Kittel-Kasuya-Yosida (RKKY) exchange. The RKKY magnetic exchange energy parameter  $J_{\text{RKKY}}$  is a Bessel function which starts at a positive value (ferromagnetic interaction) but decays fast with increasing distance between the atomic moments, crossing zero and becoming negative (antiferromagnetic interaction) at a critical distance. Therefore, when Ge starts replacing Si at the interslab sites (at  $x_p$ ), and since it has a higher atomic radius, it promotes an increase in the distance between consecutive slabs. Because of the RKKY interaction, this leads to a decrease of the magnetic exchange energy and consequently to decrease in  $T_C$ . When a critical Ge concentration limit,  $x_C$ , is reached, the RKKY interaction becomes negative and hence the AFM state becomes the most stable one. The  $x_C$  is the ferromagnetic percolation limit for these diluted systems, below which it is not possible to achieve long range ferromagnetic order. Finally, the complete analogy with the Griffiths diluted ferromagnetic system is schematized in Figure 5b.

With this set of comprehensive works the extent of the Griffiths-like behavior on the  $\text{R}_5(\text{Si},\text{Ge})_4$  compounds is shown, highlighting their magnetic nature as that of a diluted ferromagnetic system where the Ge substitution is the dilution mechanism—and hence demonstrating why the  $\text{R}_5(\text{Si},\text{Ge})_4$  are

an ideal case study for the Griffiths phase phenomenon. In addition it was found that in all the  $R_5(\text{Si,Ge})_4$  materials presenting a Griffiths-like phase [ $\text{Gd}_5(\text{Si,Ge})_4$ ;  $\text{Tb}_5(\text{Si,Ge})_4$ ;  $\text{Dy}_5(\text{Si,Ge})_4$  and  $\text{Ho}_5(\text{Si,Ge})_4$ ],  $T_G$  is systematically equal to the  $T_C$  of the O(I) phase. This has led to the conclusion that in the  $R_5(\text{Si,Ge})_4$  compounds, the low temperature phase can easily be assessed through simple measurements of magnetization as a function of temperature at constant magnetic field. In summary, it can be stated that the  $R_5(\text{Si,Ge})_4$  compounds exhibiting Griffiths-like phase are most likely to present strong competition between two phases and consequently the Griffiths-like phase constitutes a fingerprint for strong magneto-responsive properties in this family of compounds. In fact, a rapid review of the literature allows us to identify several other strongly-responsive magnetic materials, such as transition metal oxides (particularly manganites [51,52], cuprates [52] and  $\text{ACr}_2\text{X}_4$  spinels [53]) which exhibit colossal magnetoresistance and magnetoelasticity [54], magnetic semiconductors [55] and giant magnetocaloric compounds [33], all of which exhibit the Griffiths-like phase. This outcome allows us to suggest that the Griffiths-like phase can be a consequence of the strong correlation between magnetic and atomic lattices and of the strong competition between states in other materials beside the  $R_5(\text{Si,Ge})_4$  compounds. However, further investigation should be done in order to confirm this suggestion.

**Figure 5.** (a) Universal  $x,T$  phase diagram of the  $R_5(\text{Si}_x\text{Ge}_{1-x})_4$  compounds with  $R = \text{Gd}$  (triangles),  $\text{Tb}$  (squares),  $\text{Dy}$  (circles), and  $\text{Ho}$  (hexagons); (b) Adapted  $T$  vs.  $(x - x_p)$  phase diagram of a dilute FM system for the  $R_5(\text{Si}_x\text{Ge}_{1-x})_4$  system [50].



#### 4. Conclusions

In summary, in this work we have demonstrated the importance of the strong competition between phases on the origin of several giant magneto-responsive effects, particularly the magnetocaloric effect. Such competition is responsible for an additional contribution to the entropy change that can be studied thoroughly through a combination of detailed measurement/analysis of the materials magnetic properties and first principles calculations. A method to analyze the Arrott plots in order to extract the hidden magnetic ordering temperatures is reviewed and generalized. Such parameters are shown to be crucial as inputs for the simple model of the free energy as a function of temperature and for a deeper understanding on the nature of the (de)coupled magnetic and structural phase transitions. Practical examples are given, namely by explaining the coupling of magnetic and structural transitions in  $\text{Gd}_5\text{Si}_2\text{Ge}_2$  or their decoupling in the  $\text{Tb}_5\text{Si}_2\text{Ge}_2$  case. Finally, the Griffiths-like phases are reviewed in the  $\text{R}_5(\text{Si,Ge})_4$  families and a correlation between their universal phase diagram and the large magneto-responsive properties is discussed.

#### Acknowledgments

The authors acknowledge to FCT for financial support in the project PTDC/CTM-NAN/115125/2009, EXPL/EMS-ENE/2315/2013 and Projeto Norte-070124-FEDER-000070. We would also like to thank Erik Kampert, José Manue Moreira, Uli Zeitler, João Nuno Gonçalves, João Amaral, Vítor Amaral and João Bessa Sousa for the important previous discussions related with this work.

#### Author Contributions

First two authors contributed equally to this work, particularly on the writing and on the bibliographic review. André Miguel Pereira and João Pedro Araújo were responsible for this work and supervised the manuscript. Isabel T. Gomes' help was fundamental for a more clear and improved manuscript. Armandina Maria Lima Lopes, Luis Morellón, Cesar Magen, Pedro Antonio Algarabel, Manuel Ricardo Ibarra provided important inputs on the scientific analysis of the work. All authors have read and approved the final manuscript.

#### Conflicts of Interest

The authors declare no conflict of interest.

#### References

1. Miller, G.J. Complex rare-earth tetrelides,  $\text{RE}_5(\text{Si}_x\text{Ge}_{1-x})_4$ : New materials for magnetic refrigeration and a superb playground for solid state chemistry. *Chem. Soc. Rev.* **2006**, *35*, 799–813.
2. Smith, A. Who discovered the magnetocaloric effect? *Eur. Phys. J. H* **2013**, *38*, 507–517.
3. Gschneidner, K.A., Jr.; Pecharsky, V.K.; Tsokol, A.O. Recent developments in magnetocaloric materials. *Rep. Prog. Phys.* **2005**, *68*, 1479–1539.
4. Giauque, W.; MacDougall, D. Attainment of Temperatures Below  $1^\circ$  Absolute by Demagnetization of  $\text{Gd}_2(\text{SO}_4)_3 \cdot 8\text{H}_2\text{O}$ . *Phys. Rev.* **1933**, *43*, 768–768.

5. Brown, G.V. Magnetic heat pumping near room temperature. *J. Appl. Phys.* **1976**, *47*, 3673.
6. Gschneidner, K.A.; Pecharsky, V.K. Thirty years of near room temperature magnetic cooling: Where we are today and future prospects. *Int. J. Refrig.* **2008**, *31*, 945–961.
7. Brown, D.R.; Dirks, J.A.; Fernandez, N.; Stout, T.B. The Prospects of Alternatives to Vapor Compression Technology for Space Cooling and Food Refrigeration Applications. *Energ. Eng.* **2012**, *109*, 7–20.
8. Pecharsky, V.K.; Gschneidner, K.A. Giant Magnetocaloric Effect in  $Gd_5(Si_2Ge_2)$ . *Phys. Rev. Lett.* **1997**, *78*, 3–6.
9. Morellon, L.; Algarabel, P.A.; Ibarra, M.R.; Blasco, J.; Garcia-Landa, B.; Arnold, Z.; Albertini, F. Magnetic-field-induced structural phase transition in  $Gd_5(Si_{1.8}Ge_{2.2})$ . *Phys. Rev. B* **1998**, *58*, 721–724.
10. Pecharsky, V.K.; Holm, A.P.; Gschneidner, K.A.; Rink, R. Massive Magnetic-Field-Induced Structural Transformation in  $Gd_5Ge_4$  and the Nature of the Giant Magnetocaloric Effect. *Phys. Rev. Lett.* **2003**, *91*, 197204.
11. Pasquale, M.; Sasso, C.; Lewis, L.; Giudici, L.; Lograsso, T.; Schlagel, D. Magnetostructural transition and magnetocaloric effect in  $Ni_{55}Mn_{20}Ga_{25}$  single crystals. *Phys. Rev. B* **2005**, *72*, 094435.
12. Liu, J.; Gottschall, T.; Skokov, K.P.; Moore, J.D.; Gutfleisch, O. Giant magnetocaloric effect driven by structural transitions. *Nat. Mater.* **2012**, *11*, 620–626.
13. Trung, N.T.; Zhang, L.; Caron, L.; Buschow, K.H.J.; Brück, E. Giant magnetocaloric effects by tailoring the phase transitions. *Appl. Phys. Lett.* **2010**, *96*, 172504.
14. Trung, N.T.; Ou, Z.Q.; Gortenmulder, T.J.; Tegus, O.; Buschow, K.H.J.; Brück, E. Tunable thermal hysteresis in  $MnFe(P,Ge)$  compounds. *Appl. Phys. Lett.* **2009**, *94*, 102513.
15. Wada, H.; Tanabe, Y. Giant magnetocaloric effect of  $MnAs_{1-x}Sb_x$ . *Appl. Phys. Lett.* **2001**, *79*, 3302.
16. Shen, B.G.; Sun, J.R.; Hu, F.X.; Zhang, H.W.; Cheng, Z.H. Recent Progress in Exploring Magnetocaloric Materials. *Adv. Mater.* **2009**, *21*, 4545–4564.
17. Lyubina, J.; Nenkov, K.; Schultz, L.; Gutfleisch, O. Multiple Metamagnetic Transitions in the Magnetic Refrigerant  $La(Fe,Si)_{13}H_x$ . *Phys. Rev. Lett.* **2008**, *101*, 177203.
18. Ibarra, M.R.; Algarabel, P.A.; Marquina, C.; Blasco, J.; García, J. Large Magnetovolume Effect in Yttrium Doped La-Ca-Mn-O Perovskite. *Phys. Rev. Lett.* **1995**, *75*, 3541–3544.
19. Hadimani, R.L.; Bartlett, P.A.; Melikhov, Y.; Snyder, J.E.; Jiles, D.C. Field and temperature induced colossal strain in  $Gd_5(Si_xGe_{1-x})_4$ . *J. Magn. Magn. Mater.* **2011**, *323*, 532–534.
20. Morellon, L.; Stankiewicz, J.; García-Landa, B.; Algarabel, P.A.; Ibarra, M.R. Giant magnetoresistance near the magnetostructural transition in  $Gd_5Si_{1.8}Ge_{2.2}$ . *Appl. Phys. Lett.* **1998**, *73*, 3462–3464.
21. Pecharsky, V.K.; Gschneidner, K.A.; Mudryk, Y.; Paudyal, D. Making the most of the magnetic and lattice entropy changes. *J. Magn. Magn. Mater.* **2009**, *321*, 3541–3547.
22. Pecharsky, V.K.; Gschneidner, K.A., Jr.  $Gd_5(Si_xGe_{1-x})_4$ : An Extremum Material. *Adv. Mater.* **2001**, *13*, 683–686.
23. Belo, J.H.; Pereira, A.M.; Araújo, J.P.; de la Cruz, C.; dos Santos, A.M.; Gonçalves, J.N.; Amaral, V.S.; Morellon, L.; Ibarra, M.R.; Algarabel, P.A.; *et al.* Tailoring the magnetism of  $Tb_5Si_2Ge_2$  compounds by La substitution. *Phys. Rev. B* **2012**, *86*, 014403.

24. Morellon, L.; Arnold, Z.; Magen, C.; Ritter, C.; Prokhnenko, O.; Skorokhod, Y.; Algarabel, P.A.; Ibarra, M.R.; Kamarad, J. Pressure Enhancement of the Giant Magnetocaloric Effect in  $Tb_5Si_2Ge_2$ . *Phys. Rev. Lett.* **2004**, *93*, 137201.
25. Paudyal, D.; Pecharsky, V.; Gschneidner, K.; Harmon, B. Electron correlation effects on the magnetostructural transition and magnetocaloric effect in  $Gd_5Si_2Ge_2$ . *Phys. Rev. B* **2006**, *73*, 144406.
26. Paudyal, D.; Mudryk, Y.; Pecharsky, V.K.; Gschneidner, K.A. Electronic structure, magnetic properties, and magnetostructural transition in  $Tb_5Si_{2.2}Ge_{1.8}$  from first principles. *Phys. Rev. B* **2011**, *84*, 014421.
27. Pereira, A.M.; Kampert, E.; Moreira, J.M.; Zeitler, U.; Belo, J.H.; Magen, C.; Algarabel, P.A.; Morellon, L.; Ibarra, M.R.; Gonçalves, J.N.; *et al.* Unveiling the (De)coupling of magnetostructural transition nature in magnetocaloric  $R_5Si_2Ge_2$  ( $R = Tb, Gd$ ) materials. *Appl. Phys. Lett.* **2011**, *99*, 132510.
28. Mudryk, Y.; Paudyal, D.; Pecharsky, V.K.; Gschneidner, K.A.; Misra, S.; Miller, G.J. Controlling Magnetism of a Complex Metallic System Using Atomic Individualism. *Phys. Rev. Lett.* **2010**, *105*, 066401.
29. Morellon, L.; Ritter, C.; Magen, C.; Algarabel, P.; Ibarra, M. Magnetic-martensitic transition of  $Tb_5Si_2Ge_2$  studied with neutron powder diffraction. *Phys. Rev. B* **2003**, *68*, 024417.
30. Morellon, L.; Blasco, J.; Algarabel, P.A.; Ibarra, M.R. Nature of the first-order antiferromagnetic-ferromagnetic transition in the Ge-rich magnetocaloric compounds  $Gd_5(Si_xGe_{1-x})_4$ . *Phys. Rev. B* **2000**, *62*, 1022–1026.
31. Levin, E.M.; Pecharsky, V.K.; Gschneidner, K.A. Unusual Magnetic Behavior in  $Gd_5(Si_{1.5}Ge_{2.5})$  and  $Gd_5(Si_2Ge_2)$ . *Phys. Rev. B* **2000**, *62*, 625–628.
32. Casanova, F.; Batlle, X.; Labarta, A.; Marcos, J.; Mañosa, L.; Planes, A. Entropy change and magnetocaloric effect in  $Gd_5(Si_xGe_{1-x})_4$ . *Phys. Rev. B* **2002**, *66*, 100401.
33. Magen, C.; Algarabel, P.A.; Morellon, L.; Araújo, J.P.; Ritter, C.; Ibarra, M.R.; Pereira, A.M.; Sousa, J.B. Observation of a Griffiths-like Phase in the Magnetocaloric Compound  $Tb_5Si_2Ge_2$ . *Phys. Rev. Lett.* **2006**, *96*, 167201.
34. Arrott, A. Criterion for Ferromagnetism from Observations of Magnetic Isotherms. *Phys. Rev.* **1957**, *261*, 2–4.
35. Hadimani, R.L.; Melikhov, Y.; Schlagel, D.L.; Lograsso, T.A.; Jiles, D.C. Study of the Second-Order “Hidden” Phase Transition of the Monoclinic Phase in the Mixed Phase Region of  $Gd_5(Si_xGe_{1-x})_4$ . *IEEE Trans. Magn.* **2012**, *48*, 4070–4073.
36. Hadimani, R.L.; Melikhov, Y.; Snyder, J.E.; Jiles, D.C. Estimation of second order phase transition temperature of the orthorhombic phase of  $Gd_5(Si_xGe_{1-x})_4$  using Arrott plots. *J. Appl. Phys.* **2008**, *103*, 033906.
37. Pereira, A.M.; dos Santos, A.M.; Magen, C.; Sousa, J.B.; Algarabel, P.A.; Ren, Y.; Ritter, C.; Morellon, L.; Ibarra, M.R.; Araújo, J.P. Understanding the role played by Fe on the tuning of magnetocaloric effect in  $Tb_5Si_2Ge_2$ . *Appl. Phys. Lett.* **2011**, *98*, 122501.
38. Provenzano, V.; Shapiro, A.J.; Shull, R.D. Reduction of hysteresis losses in the magnetic refrigerant  $Gd_5Ge_2Si_2$  by the addition of iron. *Nature* **2004**, *429*, 853–857.

39. Carvalho, A.M.G.; Alves, C.S.; de Campos, A.; Coelho, A.A.; Gama, S.; Gandra, F.C.G.; von Ranke, P.J.; Oliveira, N.A. The magnetic and magnetocaloric properties of  $Gd_5Ge_2Si_2$  compound under hydrostatic pressure. *J. Appl. Phys.* **2005**, *97*, doi:10.1063/1.186093.
40. Liu, G.J.; Sun, J.R.; Lin, J.; Xie, Y.W.; Zhao, T.Y.; Zhang, H.W.; Shen, B.G. Entropy changes due to the first-order phase transition in the  $Gd_5Si_xGe_{4-x}$  system. *Appl. Phys. Lett.* **2006**, *88*, 212505.
41. Gschneidner, K.A.; Mudryk, Y.; Pecharsky, V.K. On the nature of the magnetocaloric effect of the first-order magnetostructural transition. *Scr. Mater.* **2012**, *67*, 572–577.
42. Svitelskiy, O.; Suslov, A.; Schlagel, D.; Lograsso, T.; Gschneidner, K.; Pecharsky, V. Elastic properties of  $Gd_5Si_2Ge_2$  studied with an ultrasonic pulse-echo technique. *Phys. Rev. B* **2006**, *74*, 184105.
43. Pecharsky, A.; Gschneidner, K.; Pecharsky, V.; Schlagel, D.; Lograsso, T. Phase relationships and structural, magnetic, and thermodynamic properties of alloys in the pseudobinary  $Er_5Si_4$ - $Er_5Ge_4$  system. *Phys. Rev. B* **2004**, *70*, 144419.
44. Pecharsky, A.O.; Pecharsky, V.K.; Gschneidner, K.A. Phase relationships and low temperature heat capacities of alloys in the  $Y_5Si_4$ - $Y_5Ge_4$  pseudo binary system. *J. Alloy. Compd.* **2004**, *379*, 127–134.
45. Belo, J.H.; Amaral, J.S.; Pereira, A.M.; Amaral, V.S.; Araujo, J.P. On the Curie temperature dependency of the magnetocaloric effect. *Appl. Phys. Lett.* **2012**, *242407*, 3–6.
46. Griffiths, R.B. Nonanalytic Behavior Above the Critical Point in a Random Ising Ferromagnet. *Phys. Rev. Lett.* **1969**, *23*, 17–19.
47. Bray, A. Nature of the Griffiths phase. *Phys. Rev. Lett.* **1987**, *59*, 586–589.
48. Zou, J.D.; Liu, J.; Mudryk, Y.; Pecharsky, V.K.; Gschneidner, K.A. Ferromagnetic ordering and Griffiths-like phase behavior in  $Gd_5Ge_{3.9}Al_{0.1}$ . *J. Appl. Phys.* **2013**, *114*, 063904.
49. Ouyang, Z.W. Griffiths-like behavior in Ge-rich magnetocaloric compounds  $Gd_5(Si_xGe_{1-x})_4$ . *J. Appl. Phys.* **2010**, *108*, 033907.
50. Pereira, A.M.; Morellon, L.; Magen, C.; Ventura, J.; Algarabel, P.A.; Ibarra, M.R.; Sousa, J.B.; Araújo, J.P. Griffiths-like phase of magnetocaloric  $R_5(Si_xGe_{1-x})_4$  ( $R = Gd, Tb, Dy, \text{ and } Ho$ ). *Phys. Rev. B* **2010**, *82*, 172406.
51. Turcaud, J.A.; Pereira, A.M.; Sandeman, K.G.; Amaral, J.S.; Morrison, K.; Berenov, A.; Daoud-Aladine, A.; Cohen, L.F. Spontaneous magnetization above  $T_c$  in  $La_{0.7}Ca_{0.3}MnO_3$  and  $La_{0.7}Ba_{0.3}MnO_3$  polycrystalline materials. *Phys. Rev. B* **2014**, in press.
52. Burgoyne, J.; Mayr, M.; Martin-Mayor, V.; Moreo, A.; Dagotto, E. Colossal Effects in Transition Metal Oxides Caused by Intrinsic Inhomogeneities. *Phys. Rev. Lett.* **2001**, *87*, 277202.
53. Oliveira, G.N.P.; Pereira, A.M.; Lopes, A.M.L.; Amaral, J.S.; dos Santos, A.M.; Ren, Y.; Mendonça, T.M.; Sousa, C.T.; Amaral, V.S.; Correia, J.G.; *et al.* Dynamic off-centering of  $Cr^{3+}$  ions and short-range magneto-electric clusters in  $CdCr_2S_4$ . *Phys. Rev. B* **2012**, *86*, 224418.
54. Michelmann, M.; Moshnyaga, V.; Samwer, K. Colossal magnetoelastic effects at the phase transition of  $(La_{0.6}Pr_{0.4})_{0.7}Ca_{0.3}MnO_3$ . *Phys. Rev. B* **2012**, *85*, 014424.

55. Guo, S.; Young, D.; Macaluso, R.; Browne, D.; Henderson, N.; Chan, J.; Henry, L.; DiTusa, J. Discovery of the Griffiths Phase in the Itinerant Magnetic Semiconductor  $\text{Fe}_{1-x}\text{Co}_x\text{S}_2$ . *Phys. Rev. Lett.* **2008**, *100*, 017209.

© 2014 by the authors; licensee MDPI, Basel, Switzerland. This article is an open access article distributed under the terms and conditions of the Creative Commons Attribution license (<http://creativecommons.org/licenses/by/3.0/>).